Model for solid-liquid and solid-solid friction of rough surfaces with adhesion hysteresis

Michael Nosonovsky[a)]
National Institute of Standards and Technology, 100 Bureau Drive, Stop 8520, Gaithersburg, Maryland 20899-8520

(Received 7 February 2007; accepted 18 April 2007; published online 11 June 2007)

Mechanisms of energy dissipation during solid-solid and solid-liquid friction are discussed. A conservative van der Waals adhesion force, when combined with surface imperfectness, such as deformation, leads to adhesion hysteresis (AH). When an asperity slides upon a substrate, the substrate is subjected to a loading-unloading cycle, and energy is dissipated due to the AH. Another mechanism, which leads to energy dissipation, involves energy barriers between metastable states due to surface roughness. Both mechanisms are fundamental for sliding and result in both solid-liquid and solid-solid friction. [DOI: 10.1063/1.2739525]

I. INTRODUCTION

The adhesion and friction at solid-liquid and solid-solid interfaces is an important topic for nanotechnology applications, because with decreasing size of application surface effects become increasingly important. The solid-liquid contact (wetting) of rough hydrophobic surfaces with water is an area of active research because of its potential applications for nanotechnology and nanomaterials. Small devices require nonsticky hydrophobic surfaces. Very hydrophobic surfaces can be obtained by increasing surface roughness. Theoretical investigation of roughness-induced hydrophobicity as well as practical design and fabrication of such surfaces has been reported recently by many authors.[1–17] The motion of a liquid droplet along a solid surface is a dissipative process, which involves adhesion between the liquid and solid. There is a general consensus in the literature that dissipation during such motion is characterized by the contact angle hysteresis (CAH) or the difference between the advancing and receding contact angles (Fig. 1). The lower the CAH, the easier the droplet can roll along the solid surface. Water-repellent surfaces, such as hydrophobic plant leaves, have low CAH. However, the origin of the CAH is still a matter of extensive debate. Several mechanisms have been suggested that lead to the CAH, including the effect of surface roughness, chemical heterogeneity, line tension, etc.[17–21]

Gao and McCarthy[20] suggested that two different mechanisms contribute simultaneously to the CAH: first, a gradual advancement of the triple line (the solid-liquid-vapor line of contact) and, second, rolling of the droplet (Fig. 1). They also argued that these two mechanisms correspond to two hierarchical levels of roughness of superhydrophobic plants leaves, which had been observed experimentally.[20] Alternative explanations of the hierarchical roughness have also been proposed by Shibuichi *et al.*,[1] who suggested that fractal roughness may lead to superhydrophobicity, Herminghaus,[4] who studied the effect of the two-tiered roughness upon pinning of the triple line, Wagner *et al.*[9] who suggested that the function of the microscale epidermal cells in the plant leaves and a superimposed layer of hydrophobic wax crystals have different functionality, Nosonovsky and Bhushan and Nosonovsky,[13,16] who showed that the hierarchical roughness may be required to maintain the stability of the liquid-air interface.

The CAH is related to the more general phenomenon known as adhesion hysteresis (AH), which is observed also during a solid-solid contact.[22–24] When two solid surfaces come in contact, the energy required to separate them is always greater than the energy gained by bringing them together, and thus the loading-unloading cycle is a thermodynamically irreversible dissipative process.[22–26] It was argued that for an adhesive dry friction the frictional shear stress is related to the AH, rather than the adhesion *per se*.[24–27] However, currently, there is no quantitative theory relating the AH with friction in a manner consistent with the experimental data.

In this work, a model is developed that takes into account two main mechanisms of frictional energy dissipation: the effects of adhesion and roughness. It is assumed that for both solid-liquid and solid-solid friction these two mechanisms are independent from each other and dominate over other possible mechanisms of friction (e.g., over the chemical interaction between surfaces or the effect of trapped wear particles or lubricating films at the interface). In particular, the model can be applied for micropatterned (textured) surfaces. For the solid-liquid friction, the model takes into account two mechanisms: the effect of the AH, which is found also at a flat surface, and advancement of the triple line through the roughness. Furthermore, using the similarity between CAH and AH during the solid-liquid and solid-solid contacts, a qualitative model for adhesive sliding and rolling friction, which relate AH and friction, is developed. Thus, a fundamental relation between solid-liquid and solid-solid friction is demonstrated. The origin of AH and its relation to surface heterogeneity (involving both the chemical heterogeneity and roughness) is also investigated.

[a)]Fax: (301) 975-5334. Electronic mail: michael.nosonovsky@nist.gov

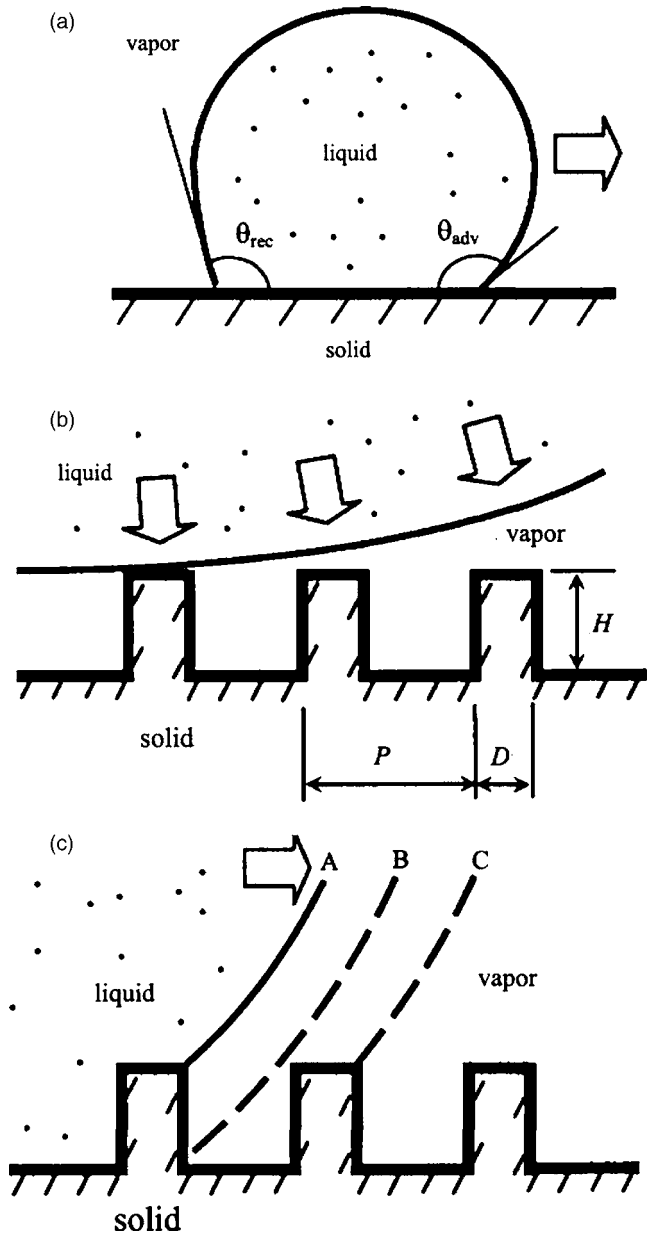

FIG. 1. (a) Schematics of advancing and receding contact angles. (b) Rolling of a droplet upon a patterned surface. (c) Advancing of the triple line and energy barriers; the position *B* has higher free energy level than *A* and *C* thus creating energy barriers.

II. SOLID-LIQUID CONTACT

In this section, the effect of AH and surface roughness upon the CAH will be studied. Young's equation relates the static contact angle of a droplet at equilibrium upon a smooth surface θ_0 to the free surface energies of the solid-liquid, solid-vapor, and liquid-vapor interfaces (γ_{SL}, γ_{SV}, and γ_{LV}, respectively),

$$\cos\theta_0 = \frac{\gamma_{SV} - \gamma_{SL}}{\gamma_{LV}}. \tag{1}$$

For a droplet in contact with a rough surface a composite solid-liquid-vapor interface can form with air pockets trapped in the valleys between the pillars. The composite interface is required for roughness-induced superhydrophobicity.[16] The total interface area then consists of the solid-liquid contact area A_{SL} and the solid-vapor contact area A_{SV}. The contact angle is given by the Cassie and Baxter[28] equation,

$$\cos\theta = R_f f_{SL}\cos\theta_0 - 1 + f_{SL}, \tag{2}$$

where $f_{SL}=A_{SL}/(A_{SL}+A_{SV})$ is fractional solid-liquid contact area, and R_f is a roughness factor defined as

$$R_f = \frac{A_{SL}}{A_F}, \tag{3}$$

where A_F is the flat solid-liquid contact area or a projection of the solid-liquid contact area A_{SL} on the horizontal plane. For a noncomposite or homogeneous interface (with no vapor pockets between the solid surface and the droplet), $f_{SL}=1$, whereas for a composite interface $0<f_{SL}<1$.

Whereas the static contact angle for a rough surface can be determined from Eq. (2), the CAH has a much more complicated nature, because there are many factors that affect it. Two main factors, which determine the CAH, are, first, the AH and, second, energy barriers created by the surface roughness and heterogeneity. Therefore, it is assumed that the CAH involves two terms: first, a term corresponding to the AH, and, second, a term corresponding to the effect of surface roughness.[17]

A. Effect of the adhesion hysteresis

When liquid comes in contact with a solid, the solid-liquid interface is created while solid-vapor and liquid-vapor interfaces are destroyed. The work of adhesion between the liquid and the solid per unit area is given by the Dupré equation,[29]

$$W = \gamma_{SV} + \gamma_{LV} - \gamma_{SL} = \gamma_{LV}(1+\cos\theta). \tag{4}$$

As it was stated earlier, the energy gained for surfaces coming to contact is greater than the energy required for their separation (or the work of adhesion) by the quantity ΔW, which constitutes the AH.[24] It is assumed that for a rough surface the CAH involves two terms: ΔW corresponding to the AH and H_r corresponding to the surface roughness. For a smooth surface, the difference between the two values of the interface energy (measured during loading and unloading) is given by ΔW_0. These two values are related to the advancing contact angle θ_{a0}, and receding contact angle θ_{r0} of the smooth surface by Eq. (4), assuming that for a smooth surface the AH is the main contributor into the CAH.

$$\cos\theta_{a0} - \cos\theta_{r0} = \frac{\Delta W_0}{\gamma_{LV}}. \tag{5}$$

For a composite interface, the fraction of the solid-liquid area is given by f_{SL}, so the AH of a rough surface ΔW is related to that of a smooth surface ΔW_0 as $\Delta W = f_{SL}\Delta W_0$, while the term that includes the surface roughness effect H_r should be added. The CAH is obtained by combining Eqs. (2)–(5),

$$\cos\theta_a - \cos\theta_r = \frac{\Delta W}{\gamma_{LV}} + H_r = \frac{f_{SL}\Delta W_0}{\gamma_{LV}} + H_r = f_{SL}(\cos\theta_{a0} - \cos\theta_{r0}) + H_r, \quad (6)$$

where θ_a and θ_r are the advancing and receding contact angles for a rough surface.[17] It is observed from Eqs. (2) and (6) that small values of f_{SL} provide both a high contact angle and a low CAH. Thus the effect of the AH is due to the change of the solid liquid area f_{SL}.

B. Effect of pinning of the triple line due to surface roughness

Now let us consider the term corresponding to the roughness H_r. During motion, the droplet passes from one metastable state to another, and these states are separated by energy barriers. For an exact theoretical calculation of the CAH, a thermodynamic analysis of energy barriers for a moving droplet would be required,[18] which is a complicated problem in the case of the three-dimensional geometry. For many practical applications, the case of microfabricated patterned surfaces with small three-dimensional pillars uniformly distributed along the surface is especially important.[10,17,30,31] The main contribution of roughness is expected to be from the sharp edges of the pillars, which may pin a moving droplet.[11] Therefore, the surface roughness term is assumed to be proportional to the density of the edges, which is equal to the perimeter of a pillar πD times number of pillars per unit area $1/P^2$.

$$H_r \propto \frac{D}{P^2}, \quad (7)$$

where D is the diameter of the pillars, and P is the pitch distance between them. It is convenient to introduce a nondimensional parameter proportionality constant c, and thus Eq. (7) is written as

$$H_r = cS_f^2 = (cD)\frac{D}{P^2}, \quad (8)$$

where $S_f = D/P$ is the nondimensional spacing factor.[16,17]

III. SOLID-SOLID CONTACT

There are several mechanisms responsible for the solid-solid friction, and adhesion is one of them. At the macroscale, the friction force is almost linearly proportional to the normal load force; however, this proportionality is attributed to the dependence of the real area of contact A_r upon the load.[32,33] The friction force F is, in turn, proportional to the real area of contact times the shear strength τ_a due to adhesion, $F = A_r\tau_a$.[34] The adhesion force between solids involves the short-distance chemical bonding forces, the long-distance van der Waals, water meniscus, and electrostatic forces.[29] For chemically nonactive surfaces in the absence of the water meniscus (e.g., in vacuum or for hydrophobic materials) and electrostatic force, the van der Waals force is the main contributor into the adhesion force.

A. van der Waals adhesion force and friction

The van der Waals force itself is conservative and does not provide a mechanism of energy dissipation. However, the AH due to surface heterogeneity and chemical reactions leads to dissipation.[24–27] Both sliding and rolling involve the creation and consequent destruction of the solid-solid interface. During such a loading-unloading cycle, the amount of energy ΔW is dissipated per unit area.

Since the underlying physical reason of the AH is in surface roughness and chemical heterogeneity, there is a natural way to obtain the hysteresis of a conservative van der Waals force by assuming that the surface is not perfectrly rigid, that is, deformable. There are a number of contact models which combine the elastic deformation and adhesion,[32,35–38] however, these theories do not address the issue of AH. We will consider a very simple model, which, however, can account for the AH.

Physically the van der Waals adhesion force and the elastic force are both caused by the atomic interaction. However, at the scale of nanometers, the contacting bodies can still be treated as a continuum, but the effects of adhesion forces are important.[32,33] The usual approach for the elastoadhesive problems is to consider the bodies in contact as a continuum media and the interaction between them to be governed by an adhesive potential. In this section we will study a simple two-dimesnsional model of the solid-solid contact with adhesion. It is expected that the two-dimensional model, while simple, can catch qualitatively the behavior during the three-dimensional contact as well.

Consider a solid continuum deformable surface in contact with a rigid cylinder with the van der Waals adhesion force acting between them [Fig. 2(a)] and the separation distance z. The cylinder presents an asperity in contact with a substrate. The total energy T of a point at the surface is given by

$$T = p(z) + W_E, \quad (9)$$

where $p(z)$ is the Lennard-Jones adhesion potential for plane surfaces,[32]

$$p_a(z) = -\frac{W}{3}\left[\left(\frac{z_0}{z}\right)^8 - 4\left(\frac{z_0}{z}\right)^2\right], \quad (10)$$

and W_E is the elastic energy, which can be approximated by

$$W_E = \frac{Ey^2}{2z_0^2}, \quad (11)$$

where y is the vertical displacement of the point (individual spring), z is the distance between the point and the rigid asperity, z_0 is the equilibrium distance, and E is the elastic modulus [Fig. 2(a)]. Equation (11) represents a simplified linear elastic law, which may be visualized as a linear spring. Combining Eqs. (9)–(11) and noting from Fig. 2(a) that $z = d - y$, where $d = R - (R^2 - x^2)^{1/2}$ is a constant distance at a given coordinate x, yields

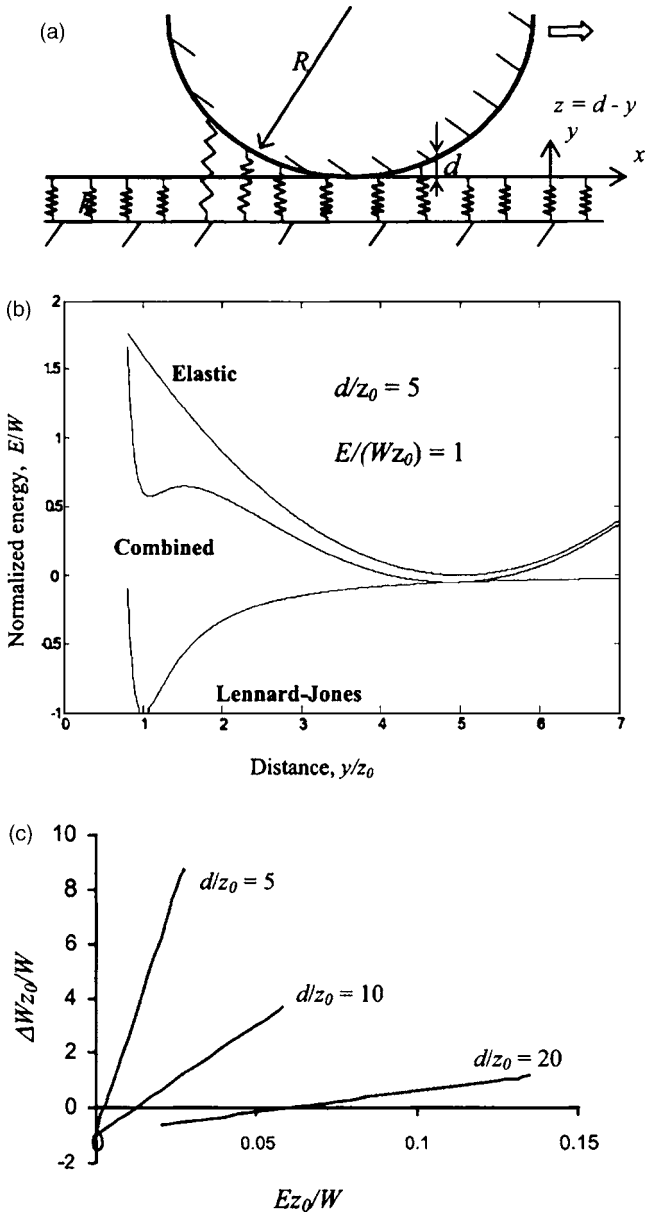

FIG. 2. (a) Schematics of a rigid spherical asperity sliding upon a deformable substrate (represented by springs), $z=d-y$, where $d=R-(R^2-x^2)^{1/2}$, with an adhesion force between them. Due to the hysteresis, the position of the springs on approach is different from that at detaching. (b) The Lennard-Jones, elastic and combined potentials, with the combined potential having two minimums. (c) Normalized energy difference of the two equilibrium states $\Delta W z_0/W$ as a function of the normalized elastic modulus $\alpha=Ez_0/W$.

$$E(z) = -\frac{W}{3}\left[\left(\frac{z_0}{z}\right)^8 - 4\left(\frac{z_0}{z}\right)^2\right] + E\frac{(d-z)^2}{2z_0^2}. \tag{12}$$

As it is observed from Fig. 2(b), the combined potential can have two minimum points, which correspond to equilibriums, and thus makes the hysteresis possible. The first equilibrium corresponds to the adhesion forces dominating over the elastic force and is achieved on approach when an element of the deformable surface "jumps to contact" with the rigid asperity. The second equilibrium corresponds to the elastic force dominating over the adhesion and is achieved at a separation when an element of the surface detaches from the asperity. The energy barriers between the two states ΔW are equal to the hysteresis. Note that even though both the adhesion and elastic forces are reversible, and the energy potential [Eq. (10)] is conservative, the hysteresis occurs in the system, which leads to a nonreversible process. The energy is consumed for excitation of elastic vibrations and waves.

The normalized energy difference of the two equilibrium states $\Delta W z_0/W$ as a function of the normalized elastic modulus $\alpha=Ez_0/W$ is presented in Fig. 2(c) for the values of the normalized distance $d/z_0=5$, 10, and 20. For $d/z_0=5$, there are two equlibriums when $0.0201<\alpha<0.1353$, which correspond to $1.01<z/z_0<1.21$ and $3.75<z/z_0<4.92$. Obviously, that the first equilibrium (near $z/z_0=1$) corresponds to the substrate, just slightly deformed by the adhesion force, whereas the second equilibrium (near $z/z_0=d/z_0=5$) corresponds to a significant deformation of the substrate, adhered to the asperity. For $d/z_0=10$, there are two equlibriums when $0.0012<\alpha<0.059$, which correspond to $1.001<z/z_0<1.187$ and $7.99<z/z_0<9.98$. For $d/z_0=20$, there are two equlibriums when $0.0001<\alpha<0.0273$, which correspond to $1.0013<z/z_0<1.1923$ and $17.51<z/z_0<19.997$. It is observed from Fig. 2(c) that the energy difference is almost linearly proportional to the normalized elastic modulus. This is because the energy of the second equilibrium (when the substrate is attached to the asperity) is greater than that of the first equlibrium, and the W_e term, which is proportional to E, dominates.

B. Shear strength due to adhesion hysteresis

Consider a rigid cylinder of radius R and length L rolling along a solid surface with the van der Waals attractive adhesion force between them. From the energy balance, when the cylinder passes the distance d, the amount of dissipated energy ΔWA_r is equal to the work of the friction force F at the distance d, and therefore, the friction force is given by

$$F = A_r \Delta W/d. \tag{13}$$

For a multiasperity contact, the real area of contact A_r is only a small fraction of the nominal contact area, which is equal to the surface area covered by the cylinder Ld.

During frictional sliding of a solid cylinder against a flat surface, the solid-solid interface is created and destroyed in a similar manner to rolling. Based on the adhesion hysteresis approach, the frictional force during sliding is also given by Eq. (13) and all considerations presented in the preceding section are valid also for the sliding friction.

However, it is well known from the experiments that the sliding friction is usually greater than the rolling friction.[34,39] This is because the plowing of asperities takes place during sliding. Even smooth surfaces have nanoasperities, and their interlocking can result in the plowing and plastic deformation of the material. Usually, asperities of a softer material are deformed by asperities of a harder material. The shear strength during plowing is often assumed to be proportional to the average absolute value of the surface slope.[39] It is therefore assumed that in addition to the adhesion hysteresis term, there is another component H_p, which is responsible for friction due to surface roughness and plowing,

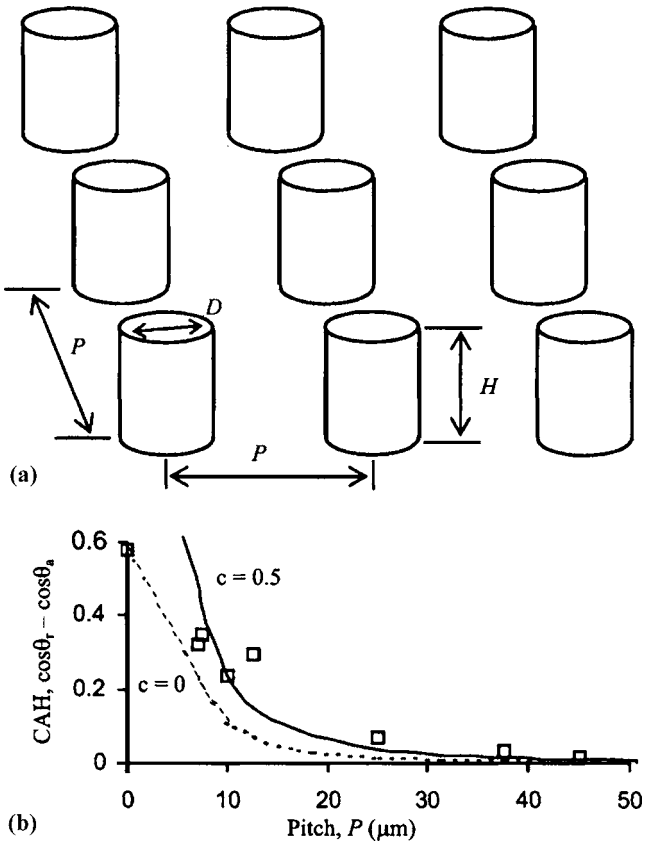

FIG. 3. (a) Schematic of a patterned superhydrophobic surface with pillars with diameter D, height H, and pitch P. (b) Contact angle hysteresis ($\cos\theta_r - \cos\theta_a$) as a function of pitch. The theoretical dependence based on the AH only ($c=0$) underestimates the CAH, whereas the theoretical dependence which includes both AH and roughness effects ($c=0.5$) provides a better fit (based on Ref. 17).

$$F = A_r(\Delta W/d + H_p). \tag{14}$$

The plowing term may be assumed to be proportional to the average absolute value of the surface slope. Note that the normal load is not included into Eq. (14) directly, however, A_r depends upon the normal load. Similarly to Eq. (6) for solid-liquid friction, the right-hand side of the Eq. (14) involves two terms: a term that is proportional to AH and a term that is proportional to roughness.

IV. DISCUSSION AND COMPARISON WITH THE EXPERIMENTAL DATA

In the preceding section, a model was presented, which relates adhesion hysteresis and surface roughness with the energy dissipation during flowing of a liquid droplet and rolling and sliding of a solid along a solid surface. A dependence of the CAH upon the distance between the pillars is presented in Fig. 3 based on Eqs. (6)–(8). For a smooth surface, the CAH is caused mostly by AH. When the pillars are introduced, the solid-liquid contact area decreases and thus the AH contribution decreases proportionally as well. However, the roughness contribution grows. With increasing pitch distance between the pillars, the roughness contribution decreases as well. It is expected that for a large pitch the pillars would not be able to support the liquid droplet, and it will collapse filling the space between the pillars and leading to the transition from the composite to the homogeneous interface, which will result in an abrupt decrease of the CAH.

An experimental study of the CAH dependence upon the pitch was conducted by Bhushan *et al.*,[17] who measured the CAH of de-ionized water sessile droplets (~5 μl) upon patterned silicon surfaces covered by a hydrophobic self-assembled monolayer of 1,1,-2,2,-tetrahydroperfluorodecyltrichlorosilane. The series of nine samples with flat-top cylindrical pillars (Fig. 3(a)) with $D=5$ μm, $H=10$ μm, and $P=7$, 7.5, 10, 12.5, 25, 37.5, 45, 60, and 75 μm was used, as well as a flat surface. For the flat surface it was found that $\theta_{a0}=116°$ and $\theta_{r0}=82°$, while for the patterned surface the CAH decreased down to $\theta_{a0}=173°$ and $\theta_{r0}=168°$. The results are shown in Fig. 3(b) plotted against the theoretically predicted values for $c=0$ (no roughness effect) and $c=0.5$ based on Eqs. (6) and (8) with $R_f=1$ (flat-top pillars) and $f_{SL}=\pi D^2/(4P^2)$. It is observed that the contribution of the AH and roughness are on the same order. Therefore, if only the AH contribution is considered, while the roughness contribution is ignored, the CAH is underestimated roughly by two times. It can be concluded that the two factors are equally important for energy dissipation during the solid-liquid contact.

Szoszkiewicz *et al.*[27] studied the correlation of nanoscale friction and adhesion hysteresis of different materials, including Pt, Au, Cu, Zn, Ti, Fe, Nb, mica, and calcite using ultrasonic force microscopy. Adhesion hysteresis was found in these experiments to scale with friction through the scaling factor containing a varying ratio of adhesion energy over the elastic modulus. This confirms the earlier observations of the correlation between the AH and friction.[22–26]

V. CONCLUSIONS

The model proposed in this paper considers two major mechanisms of friction: adhesion and the effect of the surface roughness. The origin of both solid-solid and solid-liquid friction was related to the adhesion hysteresis and surface roughness. The friction due to AH is present even at a nominally flat surface, however, the introduction of roughness increases friction. It was assumed that the effect of friction and roughness are decoupled and may be studied independently of each other, therefore, the total effect is a sum of the two components [in the right-hand parts of Eqs. (6) and (14)]. The model can be applied for the design of optimized roughness-induced superhydrophobic surfaces as well as for the control of friction using microtextured surfaces.[40] The model was developed for chemically nonactive surfaces and it takes into account the van der Waals adhesion and roughness. For the solid-liquid contact, micropatterned surfaces were studied, since these are most appropriate for applications. For the solid-solid contact, the simple case of two-dimensional surfaces was considered, because it illustrates well the dissipative mechanisms involved. A similar trend was found for the solid-solid and solid-liquid friction, and thus producing a micropatterned surface (surface texturing) that can be applied for friction reduction.

Two mechanisms that are responsible for energy dissipation during the motion of a droplet along a rough surface

have been identified. The first mechanism is the adhesion hysteresis, which leads to the energy dissipation just because new contact zones are created and destroyed during the motion. The second mechanism is related to the surface roughness, which causes pinning of the droplet at metastable states. A comparison with experimental data shows that for an artificial superhydrophobic surface contributions of both mechanisms to the contact angle hysteresis are on the same order.

The adhesion of two solid bodies is similar to the adhesion of liquid to solid and therefore the energy dissipation during the rolling of a small solid along a solid surface is similar to that during the rolling of a droplet. From the energy balance, frictional shear is equal to the AH. A simple model of the AH was developed. The model involves one rigid and one elastically deformable surface with an adhesion force between them. The adhesion potential was assumed to follow the Lennard-Jones law, whereas the deformation energy of surface was assumed to follow the second power law, which corresponds to the linearly elastic behavior. Such a system may have two equilibrium points, which results in hysteresis, because different equilibrium states are realized during loading and unloading. Thus, the combination of a conservative adhesion force with a deformable surface leads to the adhesion hysteresis and frictional energy dissipation. In a similar manner to the solid-liquid contact, the AH does not account completely for the frictional energy dissipation, and roughness plays a role. This is more pronounced for sliding friction, rather than rolling, because sliding involves more plowing and material transfer.

To summarize, the energy dissipation mechanisms of solid-liquid and solid-solid friction are similar and involve adhesion hysteresis and energy barriers caused by surface roughness. The results are consistent with the experimental data available in the literature.

[1] S. Shibuichi, T. Onda, N. Satoh, and K. Tsujii, J. Phys. Chem. **100**, 19512 (1996).
[2] M. Miwa, A. Nakajima, A. Fujishima, K. Hashimoto, and T. Watanabe, Langmuir **16**, 5754 (2000).
[3] D. Oner and T. J. McCarthy, Langmuir **16**, 7777 (2000).
[4] S. Herminghaus, Europhys. Lett. **52**, 165 (2000).
[5] C. W. Extrand, Langmuir **22**, 1711 (2006).
[6] H. Y. Erbil, A. L. Demirel, and Y. Avci, Science **299**, 1377 (2003).
[7] A. Marmur, Langmuir **19**, 8343 (2003).
[8] A. Lafuma and D. Quéré, Nat. Mater. **2**, 457 (2003).
[9] P. Wagner, F. Furstner, W. Barthlott, and C. Neinhuis, J. Exp. Bot. **54**, 1295 (2003).
[10] B. He, N. A. Patankar, and J. Lee, Langmuir **19**, 4999 (2003).
[11] M. Nosonovsky and B. Bhushan, Microsyst. Technol. **11**, 535 (2005).
[12] M. Nosonovsky and B. Bhushan, Microsyst. Technol. **12**, 273 (2006).
[13] M. Nosonovsky and B. Bhushan, Ultramicroscopy (in press).
[14] W. Li and A. Amirfazli, J. Colloid Interface Sci. **292**, 195 (2006).
[15] E. Bormashenko, T. Stein, G. Whyman, Y. Bormashenko, and E. Pogreb, Langmuir **22**, 9982 (2006).
[16] M. Nosonovsky, Langmuir **23**, 3157 (2007).
[17] B. Bhushan, M. Nosonovsky, and Y.-C. Jung, J. R. Soc., Interface (in press).
[18] R. E. Johnson and R. H. Dettre, Adv. Chem. Ser. **43**, 112 (1964).
[19] A. Marmur, Adv. Colloid Interface Sci. **50**, 121 (1994).
[20] L. Gao and T. J. McCarthy, Langmuir **22**, 2966 (2006).
[21] B. Krasovitski and A. Marmur, Langmuir **21**, 3881 (2005).
[22] Y. L. Chen, C. A. Helm, and J. Israelachvili, J. Phys. Chem. **95**, 10736 (1991).
[23] H. Yoshizawa, Y. L. Chen, and J. Israelachvili, J. Phys. Chem. **97**, 4128 (1993).
[24] M. Ruths, A. D. Berman, and J. N. Israelachvili, *Nanotribology and Nanomechanics: An Introduction* (Springer, New York, 2005), pp. 389–482.
[25] N. Maeda, N. Chen, N. Tirrell, and J. N. Israelachvili, Science **297**, 379 (2002).
[26] H. B. Zeng, M. Tirrell, and J. Israelachvili, J. Adhes. **82**, 933 (2006).
[27] R. Szoszkiewicz, B. Bhushan, and B. D. Huey, J. Chem. Phys. **122**, 144708 (2005).
[28] A. Cassie and S. Baxter, Trans. Faraday Soc. **40**, 546 (1944).
[29] J. N. Israelachvili, *Intermolecular and Surface Forces*, 2nd ed. (Academic, London, 1992).
[30] R. Fürstner, W. Barthlott, C. Neinhuis, and P. Walzel, Langmuir **21**, 956 (2005).
[31] Z. Burton and B. Bhushan, Nano Lett. **5**, 1607 (2005).
[32] K. L. Johnson, Tribol. Int. **31**, 413 (1998).
[33] G. G. Adams and M. Nosonovsky, Tribol. Int. **33**, 441 (2000).
[34] F. P. Bowden and D. Tabor, *The Friction and Lubrication of Solids* (Clarendon, Oxford, 1950).
[35] K. L. Johnson, K. Kendall, and A. D. Roberts, Proc. R. Soc. London, Ser. A **324**, 301 (1971).
[36] B. V. Derjaguin, V. M. Muller, and Yu. P. Toporov, J. Colloid Interface Sci. **53**, 314 (1975).
[37] G. A. D. Briggs and B. J. Briscoe, J. Phys. D **10**, 2453 (1977).
[38] O. T. Sari, G. G. Adams, and S. Muftu, ASME J. Appl. Mech. **72**, 633 (2005).
[39] B. Bhushan, *Introduction to Tribology* (Wiley, New York, 2002).
[40] I. Etsion, ASME J. Tribol. **127**, 248 (2005).